

# Unambiguous Delay-Doppler Recovery from Random Phase Coded Pulses

Xiang Liu, Deborah Cohen, Tianyao Huang, Yimin Liu, Yonina C. Eldar

**Abstract**—Pulse Doppler radars suffer from range-Doppler ambiguity that translates into a trade-off between maximal unambiguous range and velocity. Several techniques, like the multiple PRFs (MPRF) method, have been proposed to mitigate this problem. The drawback of the MPRF method is that the received samples are not processed jointly, decreasing signal to noise ratio (SNR). To overcome the drawbacks of MPRF, we employ a random pulse phase coding approach to increase the unambiguous range region while preserving the unambiguous Doppler region. Our method encodes each pulse with a random phase, varying from pulse to pulse, and then processes the received samples jointly to resolve the range ambiguity. This technique increases the SNR through joint processing without the parameter matching procedures required in the MPRF method. The recovery algorithm is designed based on orthogonal matching pursuit so that it can be directly applied to either Nyquist or sub-Nyquist samples. The unambiguous delay-Doppler recovery condition is derived with compressed sensing theory in noiseless settings. In particular, an upper bound to the number of targets is given, with respect to the number of samples in each pulse repetition interval and the number of transmit pulses. Simulations show that in both regimes of Nyquist and sub-Nyquist samples our method outperforms the popular MPRF approach in terms of hit rate.

## I. INTRODUCTION

Pulse Doppler radars, which simultaneously estimate targets' range and velocity, are widely used for both civilian and military purposes, including meteorological applications [1], [2], surveillance and tracking systems [3]. However, such systems suffer from the so-called “range-Doppler ambiguity dilemma” [1], [2]. For a certain pulse repetition interval (PRI)  $T_r$ , the maximum unambiguous range is  $R_{\max} = cT_r/2$ , where  $c$  is the velocity of the light, and the maximum unambiguous velocity is  $V_{\max} = \lambda/(4T_r)$ , where  $\lambda$  is the radar wavelength. This fundamental problem creates a trade-off between range and velocity ambiguity and limits their product to  $R_{\max}V_{\max} = c\lambda/8$ .

Several techniques have been proposed over the years to mitigate this problem by increasing either the unambiguous

velocity region or the unambiguous range region. A first approach uses carrier frequency variation and transmits pulses with different carriers. The velocity ambiguous region is increased by exploiting phase differences between pairs of reflected pulses [4]. However, it is not clear how to compute the phase differences in the presence of more than one target. This technique suffers from additional issues, including radar cross section (RCS) variation under different carriers and large frequency excursion requirement [5]. Therefore, methods based on pulse repetition frequency (PRF) variation are generally preferred [3], where  $\text{PRF} = 1/T_r$ .

Two main PRF variation based techniques are staggered PRFs and multiple PRFs (MPRF). The use of staggered PRFs has been essentially proposed to raise the first blind speed  $V_{\max}$  significantly without degrading unambiguous range [6]. Pulse-to-pulse stagger varies the PRF from one pulse to the next pulse, achieving increased Doppler coverage [7], [8]. The main disadvantage of this approach is that the data corresponds to a non-uniformly sampled sequence, making it more difficult to apply coherent Doppler filtering [6]. In addition, clutter cancellation also becomes more challenging and the sensitivity to noise increases [3], [4].

The MPRF approach transmits several pulse trains, each with a different PRF. Ambiguity resolution is typically achieved by searching for coincidence between unfolded Doppler or delay estimations for each PRF. A popular approach, adopted in [9], relies on the Chinese Remainder Theorem [10] and uses two PRFs, such that the numerator and denominator of the ratios between these are prime numbers. The ambiguous ranges are computed for each train and congruence between these are found by exhaustive search. However, in this approach, a small range error on a single PRF can cause a large error in the resolved range with no indication that this has happened [11].

Trunk et. al [11] propose a clustering algorithm which implements the search of a matching interval by computing average distances to cluster centers. This technique still requires exhaustive search of clusters and does not process the samples jointly, decreasing signal to noise ratio (SNR). An alternative method using a maximum likelihood criterion, which avoids the use of matching intervals, has been proposed for Doppler ambiguity resolution [3]. This algorithm, which relies on the choice of particular values for the PRFs, first estimates the folded or reduced frequency and then uses it to estimate the ambiguity order. However, it has been demonstrated that the ambiguity order estimation is very sensitive to the folded frequency estimation performed initially [8].

In this paper, we adopt a random pulse phase coding (RPPC)

This project is funded by the National Natural Science Foundation of China under Grants No. 61801258, European Union's Horizon 2020 research and innovation program under grant agreement No. 646804-ERC-COG-BNYQ, from the Air Force Office of Scientific Research under grant No. FA9550-18-1-0208. Deborah Cohen is grateful to the Azrieli Foundation for the award of an Azrieli Fellowship.

Y. C. Eldar is with the Faculty of Mathematics and Computer Science, Weizmann Institute of Science, Rehovot, Israel (e-mail: yonina.eldar@weizmann.ac.il).

D. Cohen was with the Faculty of Electrical Engineering, Technion - Israel Institute of Technology, Haifa, Israel, when performing part of this work, and is now with Google Research, Tel Aviv, Israel.

T. Huang, Y. Liu, and X. Liu are with the Department of Electronic Engineering, Tsinghua University, Beijing, China.

approach to increase the unambiguous range region, while preserving the unambiguous Doppler region and using a single PRF. RPPC has been used in polarimetric weather radars, which exploit the inherent random phase between pulses of the popular magnetron transmitters [12]. In this context, RPPC mitigates out-of-trip echoes [12]. In our approach, a random phase is introduced from pulse to pulse, and we then jointly process the received signals from all pulses to resolve range ambiguity.

Our work has three main contributions. First, theoretical analysis is performed on unambiguous target recovery conditions in the noiseless case. For a given ambiguous delay region  $[0, QT_r)$  with an integer  $Q > 1$ , it is proved that range ambiguity can be resolved with sparse recovery methods if the number of targets in each ambiguous range resolution bin is less than  $(P - Q + 2)/2$ , where  $P$  is the number of transmit pulses. Second, compared with the MPRF methods, our approach improves the SNR by jointly processing the samples from the overall received signal, rather than matching the estimated parameters from each pulse train processed separately. Therefore, our approach achieves better performance of delay estimation than the MPRF methods. Finally, we provide a systematic delay-Doppler recovery algorithm based on orthogonal matching pursuit (OMP) [13], [14] which does not involve exhaustive search. From a practical point of view, our method does not require the use of different PRFs, simplifying hardware implementation.

In addition, our recovery algorithm can be directly applied to compressed samples, obtained using the sub-Nyquist method proposed in [15]–[17]. This scheme exploits the sparse nature of radar target scenes to overcome the sampling rate bottleneck, breaking the link between radar signal bandwidth and sampling rate. In [15]–[17], the Fourier coefficients of the received signal are obtained from low-rate point wise samples taken after analog pre-filtering. The delay-Doppler map may then be recovered using compressed sensing (CS) algorithms [18], [19]. Our unambiguous delay-Doppler recovery algorithm can be applied to these compressed samples, without requiring any modification. Given the number of samples  $K$  with in each PRI, an upper bound to the number of targets for unambiguous target recovery is given by  $\min\{(K + 1)/2, (P - Q + 2)/2\}$ .

We compare our approach to the popular MPRF method of [11], which has been shown to outperform the matching interval scheme based on the Chinese Remainder Theorem. We demonstrate that our algorithm outperforms the MPRF approach both in Nyquist and sub-Nyquist regimes.

The rest of the paper is organized as follows. In Section II, we present the random phase coded pulse radar model with range ambiguity, introduce the corresponding sampling methods, and establish the range-Doppler recovery model. Section III introduces our unambiguous delay-Doppler recovery algorithm based on OMP. Section IV presents a theoretical analysis on the unambiguous delay-Doppler recovery in the noiseless case. Simulation results are provided in Section V. Section VI draws a brief conclusion.

*Notation:* For a vector  $\mathbf{x}$ , a matrix  $\mathbf{X}$ , and positive integers  $i$  and  $j$ , the  $i$ -th element of  $\mathbf{x}$  is denoted by  $x_i$ , the  $j$ -th column

of  $\mathbf{X}$  is denoted by  $\mathbf{X}_j$ , and the  $(i, j)$ -th element of  $\mathbf{X}$  is written as  $X_{i,j}$ . Here, the element index begins with zero. For instance, the first element of  $\mathbf{x}$  is  $x_0$ , and the first column of  $\mathbf{X}$  is  $\mathbf{X}_0$ . Given a positive integer  $N$ ,  $W_N$  represents  $e^{-j2\pi/N}$ . In this paper,  $(\cdot)^H$ ,  $(\cdot)^T$ ,  $(\cdot)^c$  and  $(\cdot)^{-1}$  are the Hermitian transpose, transpose, conjugate and inverse, respectively.

## II. PROBLEM FORMULATION

In this section, we first present the signal model of random phase coded pulse radar. Then, we introduce the sampling schemes for radar echoes, in both Nyquist and sub-Nyquist regimes. Finally, we formulate the sparse matrix recovery problem for range-Doppler recovery, which will be used to derive the recovery method and recovery conditions in the following sections.

### A. Signal model

In the signal model, a pulse-Doppler radar transceiver transmits a phase-coded pulse train consisting of  $P$  equally spaced pulses. For  $0 \leq t \leq PT_r$ , this pulse train is given by

$$s(t) = \sum_{p=0}^{P-1} h(t - pT_r) e^{j\phi[p]} e^{j2\pi f_c t}, \quad (1)$$

where  $h(t)$  is the time-limited baseband waveform taking nonzero values in the interval  $[0, T_h)$  (with  $T_h$  being the pulse width), the pulse-to-pulse delay  $T_r$  is the PRI, and  $f_c$  is the carrier frequency. We use  $\phi[p]$  to represent the phase shift of the  $p$ -th pulse, for  $p = 0, \dots, P - 1$ . As opposed to the traditional pulse Doppler radar, where the phase codes are identical, here in the random phase coded pulse radar,  $\phi[p]$  is randomly distributed in the interval  $[0, 2\pi)$  and varies from pulse to pulse. The entire span of the signal in (1) is called the coherent processing interval (CPI). We also assume that  $h(t)$  is band-limited with negligible energy at frequencies beyond  $B_h/2$ , and  $B_h$  is referred to as the bandwidth of  $h(t)$ .

To derive the received radar signal, we first consider a point target. Given the target's distance  $R$  and relative radial velocity to the radar  $V$ , the radar receiver receives

$$\begin{aligned} r(t) &= s(t - 2(R + Vt)/c) \\ &= \sum_{p=0}^{P-1} h(t - pT_r - \tau - 2vt/c) e^{j2\pi f_c (t - \tau - 2vt/c)} e^{j\phi[p]} + u(t), \end{aligned} \quad (2)$$

where  $\tau = 2R/c$  is the time delay,  $u(t)$  is the additive noise and the amplitude of the signal is ignored. Under the assumption that the target does not move across range resolution bins during the CPI, the signal after down-converting is

$$r_d(t) = \sum_{p=0}^{P-1} h(t - pT_r - \tau) e^{-j2\pi f_c \tau} e^{-j2\pi vt} e^{j\phi[p]} + u_d(t), \quad (3)$$

where  $\nu = 2v f_c / c$  is the Doppler frequency and  $u_d(t)$  is the additive noise.

Then we consider a target scene where  $L$  non-fluctuating point targets satisfying the Swerling-0 model [10] locates within the radar coverage region. The  $l$ -th target is defined by three parameters: a time delay  $\tilde{\tau}_l = 2R_l/\tau$ , where  $R_l$  is

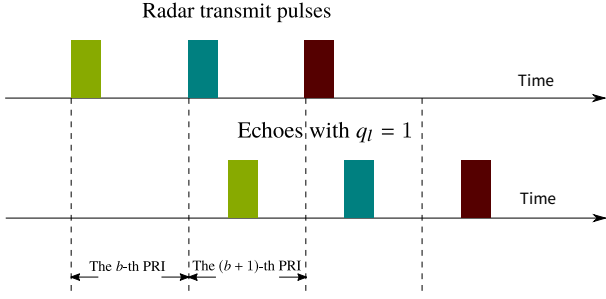


Fig. 1. The pulse transmitted in the  $b$ -th PRI is received in the  $(b+1)$ -th PRI.

the relative distance from the radar to the target; a Doppler frequency  $\nu_l = 2V_l/\lambda$ , where  $V_l$  is the relative radial velocity of the target; and a complex amplitude of the echo signal  $\alpha_l$ . The targets are defined in the radar radial coordinate system and the Doppler frequencies are assumed to lie in the unambiguous frequency region, that is  $|\nu_l| < 1/(2T_r)$ , for  $l = 0, \dots, L-1$ . As opposed to the common assumption in traditional radars, the time delays  $\tilde{\tau}_l$  are not assumed to lie in the unambiguous region, namely less than the PRI  $T_r$ , but may exceed  $T_r$ , and range ambiguity occurs for a conventional pulse Doppler radar. For convenience, we decompose  $\tilde{\tau}_l$  into its integer part (the ambiguity order)  $q_l$  and the fractional part (the folded or reduced delay)  $\tau_l$  as

$$\tilde{\tau}_l = \tau_l + q_l T_r, \quad (4)$$

where  $q_l \geq 0$  is an integer and  $0 \leq \tau_l < T_r$ .

From (3), the received signal after down-converting is written as

$$y(t) = \sum_{l=0}^{L-1} \sum_{p=0}^{P-1} \bar{\alpha}_l h(t - \tau_l - (p + q_l)T_r) e^{-j2\pi\nu_l t} e^{j\phi[p]} + u_d(t), \quad (5)$$

for  $0 \leq t \leq PT_r$ , where  $\bar{\alpha}_l = \alpha_l e^{-j2\pi f_c \tilde{\tau}_l}$  and  $u_d(t)$  is additive noise. Pulse Doppler radars usually transmit pulses with low duty cycle, i.e.  $T_h \ll T_r$ , and hence  $y(t)$  can be approximated as

$$y(t) = \sum_{l=0}^{L-1} \sum_{p=0}^{P-1} \tilde{\alpha}_l h(t - \tau_l - (p + q_l)T_r) e^{-j2\pi\nu_l(p+q_l)T_r} e^{j\phi[p]} + u_d(t), \quad (6)$$

for  $0 \leq t \leq PT_r$ , where  $\tilde{\alpha}_l = \bar{\alpha}_l e^{j2\pi\nu_l \tau_l}$ .

For convenience, we rewrite the overall received signal (6) with respect to each PRI. Note that in traditional pulse Doppler settings, namely under the assumption that  $0 \leq \tilde{\tau}_l < T_r$ , the  $p$ -th pulse reflected from the targets is received in the  $p$ -th PRI. Here, the  $p$ -th pulse reflected from the  $l$ -th target is received in the  $(p + q_l)$ -th PRI. Figure 1 illustrates this phenomenon for  $q_l = 1$ , in which the  $b$ -th pulse is received in the  $(b+1)$ -th PRI. In other words, the  $(b - q_l)$ -th pulse reflected from the

$l$ -th target is received in the  $b$ -th PRI. Substituting  $p = b - q_l$ , we can then rewrite (6) as

$$\begin{aligned} y(t) &= \sum_{l=0}^{L-1} \sum_{b=q_l}^{P+q_l-1} \tilde{\alpha}_l h(t - \tau_l - b\tau) e^{-j2\pi\nu_l b\tau} e^{j\phi[b-q_l]} + u_d(t) \\ &= \sum_{b=0}^{P-1} \sum_{l=0}^{L-1} \tilde{\alpha}_l h(t - \tau_l - b\tau) e^{-j2\pi\nu_l b\tau} z[b - q_l] + u_d(t), \end{aligned} \quad (7)$$

for  $0 \leq t \leq PT_r$ , where the sequence  $\{z[p]\}$  is defined as

$$z[p] = \begin{cases} e^{j\phi[p]}, & \text{for } p = 0, \dots, P-1, \\ 0, & \text{for } p < 0 \text{ or } p > P-1. \end{cases} \quad (8)$$

From (7), the received signal in the  $b$ -th PRI is expressed as

$$y_b(t) = \sum_{l=0}^{L-1} \tilde{\alpha}_l h(t - \tau_l - b\tau) e^{j2\pi\nu_l b\tau} z[b - q_l] + u_b(t), \quad (9)$$

for  $b = 0, 1, \dots, P-1$  and  $b\tau \leq t < (b+1)\tau$ .

Given the received signal  $y_b(t)$ ,  $b = 0, \dots, P-1$ , our goal is to recover the range and velocity of targets, namely the time delays  $\{\tilde{\tau}_l\}$  and Dopplers  $\{\nu_l\}$ ,  $l = 0, \dots, L-1$ . To recover these parameters with digital processors, we will first sample the signal, as presented in the next subsection.

### B. Sub-Nyquist sampling

To reduce the sampling rates, we apply sub-Nyquist sampling in fast time, namely sampling the signal in each PRI with sampling rate lower than the bandwidth  $B_h$ . Generally, aliasing of frequency bands will occur if the sampling rate is below the signal bandwidth. Nevertheless, the proposed techniques for sub-Nyquist radar [15]–[17] can obtain the necessary frequency information to recover target parameters without aliasing, by appropriate analog anti-aliasing filtering before sub-Nyquist sampling.

To see this, we compute the Fourier series representation of the aligned received signal in the  $b$ -th PRI  $y_b(t + b\tau)$  with respect to the period  $[0, \tau)$ . This result in [15], [16]

$$\begin{aligned} Y_b[m] &= \frac{1}{\tau} H\left(\frac{2\pi m}{\tau}\right) \sum_{l=0}^{L-1} \tilde{\alpha}_l e^{-j2\pi\nu_l b\tau} e^{-j\frac{2\pi}{\tau} m\tau_l} z[b - q_l] + U_b[m], \end{aligned} \quad (10)$$

for  $m = 0, \dots, N-1$ , where  $H(\cdot)$  denotes the Fourier transform of  $h(t)$ ,  $N = \lfloor B_h \tau \rfloor$  is the number of Fourier samples, and  $\{U_b[m]\}$  are the Fourier series coefficients of  $u_b(t + b\tau)$ . Here,  $\lfloor \cdot \rfloor$  represents the floor function. For convenience, let

$$\begin{aligned} \tilde{Y}_b[m] &= \frac{\tau Y_b[m]}{H(2\pi m/\tau)} \\ &= \sum_{l=0}^{L-1} \tilde{\alpha}_l e^{-j2\pi\nu_l b\tau} e^{-j\frac{2\pi}{\tau} m\tau_l} z[b - q_l] + \tilde{U}_b[m] \end{aligned} \quad (11)$$

be the normalized Fourier series of the  $b$ -th PRI, where  $\tilde{U}_b[m] = \tau U_b[m]/H(2\pi m/\tau)$ .

From (11), the target parameters  $\{\tau_l, \nu_l, q_l\}$  are contained in the normalized Fourier series  $\tilde{Y}_b[k]$ . To recover the target parameters, sub-Nyquist radar obtains the Fourier series from

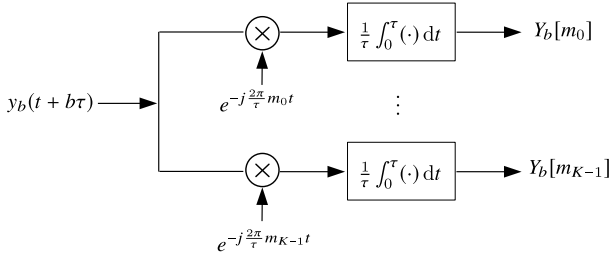


Fig. 2. In Xampling [17], the Fourier series is directly sampled after analog pre-processing in each channel.

low rate samples of the received signal in each PRI. In this paper, we consider the Xampling [20], [21] based sub-Nyquist radar systems. For each PRI, Xampling allows one to generate an arbitrary subset

$$\kappa = \{m_0, \dots, m_{K-1}\} \subset \{0, \dots, N-1\},$$

comprised of  $K = |\kappa|$  frequency components, and obtain the corresponding Fourier coefficients  $Y_b[m_k]$ , for  $k = 0, \dots, K-1$ , from  $K$  point-wise samples of the received signal  $y_b(t + b\tau)$  after appropriate analog pre-processing. The procedure of Xampling is shown in Fig. 2, in which the received signal is split into  $K = |\kappa|$  channels. In the  $k$ -th channel,  $y_b(t + b\tau)$  is first mixed with the harmonic signal  $e^{-j(2\pi/\tau)m_k t}$ , integrated over the aligned receive window  $[0, \tau)$ , and then sampled at a low rate.

After sub-Nyquist sampling, the problem is to recover the targets' delays  $\{\hat{\tau}_l\}$  and Dopplers  $\{\nu_l\}$ , from the compressed normalized Fourier series

$$\tilde{Y}_b[m_k] = \sum_{l=0}^{L-1} \tilde{\alpha}_l e^{-j2\pi\nu_l b\tau} e^{-j\frac{2\pi}{\tau}m_k \tau_l} z[b - q_l] + \tilde{U}_b[m_k], \quad (12)$$

for  $b = 0, \dots, P-1$  and  $k = 0, \dots, K-1$ .

### C. Matrix formulation

In this subsection, we recast (12) in a matrix formulation. To that aim, we assume that the delays and Dopplers of the  $L$  targets lie on the center of delay resolution bins and Doppler resolution bins, respectively. As in traditional pulse Doppler radar, the size of a delay resolution bin is  $\tau/N$ , while that of a Doppler resolution bin is  $1/(P\tau)$ . Then the delays and Doppler can be represented by  $\tau_l = n_l\tau/N$  and  $\nu_l = p_l/(P\tau)$ , where  $n_l$  and  $p_l$  are integers in the intervals  $[0, N-1]$  and  $[0, P-1]$ , respectively, for  $l = 0, \dots, L-1$ . Under this assumption, (12) becomes

$$\tilde{Y}_b[m_k] = \sum_{l=0}^{L-1} \tilde{\alpha}_l W_P^{bp_l} W_N^{m_k n_l} z[b - q_l] + \tilde{U}_b[m_k], \quad (13)$$

for  $b = 0, \dots, P-1$  and  $k = 0, \dots, K-1$ , where  $W_P^{bp_l} = e^{-j2\pi b p_l / P}$  and  $W_N^{m_k n_l} = e^{-j2\pi m_k n_l / N}$ .

Define the ambiguity factor

$$Q = \max(q_0, \dots, q_{L-1}) + 1. \quad (14)$$

When  $Q = 1$ , there is no range ambiguity. In our model, range ambiguity is considered, i.e.  $Q > 1$ . In (13), the target

parameters  $\{\tilde{\alpha}_l, n_l, q_l, p_l\}$  can be characterized by a matrix  $\tilde{\mathbf{X}} \in \mathbb{C}^{N \times PQ}$ , which is defined as

$$\tilde{\mathbf{X}}_{n,c} = \begin{cases} \tilde{\alpha}_l, & \text{if } n = n_l \text{ and } c = Pq_l + p_l, \\ 0, & \text{otherwise.} \end{cases} \quad (15)$$

In other words, the matrix  $\tilde{\mathbf{X}}$  is an  $N \times PQ$  matrix which contains the value  $\tilde{\alpha}_l$  at the corresponding  $L$  indexes  $(n_l, Pq_l + p_l)$ , for  $l = 0, \dots, L-1$ , while the rest of the elements in  $\tilde{\mathbf{X}}$  are all zeros.

We may now rewrite (13) into a matrix observation model

$$\mathbf{Y} = \mathbf{A} \tilde{\mathbf{X}} \mathbf{B}^T + \mathbf{U}, \quad (16)$$

where the  $(k, b)$ -th entry of  $\mathbf{Y} \in \mathbb{C}^{K \times P}$  is given by  $\tilde{Y}_b[m_k]$ , denoting the  $k$ -th Fourier series of the radar signal received in the  $b$ -th PRI, for  $b = 0, \dots, P-1$  and  $k = 0, \dots, K-1$ ; the partial Fourier matrix  $\mathbf{A} \in \mathbb{C}^{K \times N}$  has the  $(k, n)$ -th entry given by  $W_N^{m_k n}$ , representing the fast-time frequency response from the  $n$ -th range resolution bin at the frequency point  $m_k/\tau$ , for  $n = 0, \dots, N-1$  and  $k = 0, \dots, K-1$ ; and  $\mathbf{U} \in \mathbb{C}^{K \times P}$  is the additive noise whose  $(k, b)$ -th entry is given by  $\tilde{U}_b[m_k]$ .

In (16), the matrix  $\mathbf{B} \in \mathbb{C}^{P \times PQ}$  consists of  $Q$  blocks. Particularly,  $\mathbf{B}$  is represented by

$$\mathbf{B} = [\mathbf{B}^{(0)}, \mathbf{B}^{(1)}, \dots, \mathbf{B}^{(Q-1)}], \quad (17)$$

where  $\mathbf{B}^{(q)} \in \mathbb{C}^{P \times P}$ , and the  $(b, p)$ -th entry of  $\mathbf{B}^{(q)}$  is given by  $W_P^{bp} z[b - q]$ , for  $p = 0, \dots, P-1$  and  $b = 0, \dots, P-1$ . Here, each block  $\mathbf{B}^{(q)}$  represents the slow-time response of the targets with ambiguity order  $q$ .

From the matrix formation model (16),  $\tilde{\mathbf{X}}$  should be a solution of the following equation

$$\mathbf{A} \mathbf{X} \mathbf{B}^T = \mathbf{Y}, \quad (18)$$

in the noiseless case. The problem is to recover the sparse matrix  $\tilde{\mathbf{X}}$  from the observation  $\mathbf{Y}$  and measurement matrix  $\mathbf{A}$  and  $\mathbf{B}$ , by finding the solution of (18). For a Nyquist pulse-Doppler radar without range ambiguity, namely  $K = N$  and  $Q = 1$ ,  $\mathbf{A}$  and  $\mathbf{B}$  are full-rank square matrices, so the solution to (18) is unique. However, in our setting, namely  $K \leq N$  and  $Q > 1$ , due to the rank deficiency of  $\mathbf{A}$  and  $\mathbf{B}$ , (18) is an underdetermined equation and may not have a unique solution. Nevertheless, when  $L \ll NPQ$ , there are only a few nonzero elements in  $\tilde{\mathbf{X}}$ , which means that  $\tilde{\mathbf{X}}$  is a sparse matrix. We can use sparse matrix recovery to recover  $\tilde{\mathbf{X}}$  from the received signal, as discussed in the following section.

### III. DELAY-DOPPLER RECOVERY METHODS

To recover  $\tilde{\mathbf{X}}$  from (16), we consider the  $\ell_0$  "norm" minimization problem

$$\min \|\mathbf{X}\|_0, \quad \text{s.t. } \mathbf{A} \mathbf{X} \mathbf{B}^T = \mathbf{Y}, \quad (19)$$

under the assumption that  $\mathbf{X}$  is a sparse matrix. Here,  $\|\cdot\|_0$  represents  $\ell_0$  "norm", which is defined as the number of nonzero elements of a vector or a matrix. The  $\ell_0$  "norm" is a non-convex function and the sparse matrix recovery problem (19) is generally NP hard. Therefore, solving (19) is computationally intractable in practical problems. A more practical way is to compute a sub-optimal solution with heuristic greedy methods

such as OMP [14], or with convex relaxation based approaches such as iterative shrinkage-thresholding [22], [23].

We use the matrix version of OMP [13], [24] to solve (19) and the procedures are shown in Algorithm 1. In each iteration of Algorithm 1, the maximal projection of the observation matrix onto the measurement matrices is retained. In the  $t$ -th iteration of Algorithm 1,  $\mathbf{D}^{(t)}$  is a  $t \times t$  matrix whose  $(p, q)$ -th entry is given by

$$[\mathbf{D}^{(t)}]_{p,q} = \mathbf{A}_{\lambda_p(1)}^H \mathbf{A}_{\lambda_q(1)} \mathbf{B}_{\lambda_q(2)}^T \mathbf{B}_{\lambda_p(2)}^c, \quad (20)$$

for  $1 \leq p, q \leq t$ , and  $\mathbf{d}^{(t)}$  is a  $t \times 1$  vector whose  $p$ -th element is given by

$$[\mathbf{d}^{(t)}]_p = \mathbf{A}_{\lambda_p(1)}^H \mathbf{Y} \mathbf{B}_{\lambda_p(2)}^c, \quad (21)$$

for  $1 \leq p \leq t$ . Once  $\mathbf{X}$  is recovered, the delay ambiguity orders, folded delays and Dopplers are estimated as

$$\hat{q}_l = \left\lfloor \frac{[\Lambda_l]_2}{P} \right\rfloor, \quad \hat{\tau}_l = \frac{\tau}{N} [\Lambda_l]_1, \quad \hat{\nu}_l = \frac{[\Lambda_l]_2 - \hat{q}_l P}{P\tau}, \quad (22)$$

where  $\lfloor \cdot \rfloor$  is the floor function and  $\Lambda_l$  is the  $l$ -th element of  $\Lambda$ .

---

**Algorithm 1** OMP for sparse matrix recovery

---

**Input:**

- Observation matrix  $\mathbf{Y}$ ;
- Measurement matrices  $\mathbf{A}$  and  $\mathbf{B}$ ;
- Number of non-zero elements  $L$  in the sparse matrix.

**Output:**

- Support set  $\Lambda$  containing the locations of non zero indices of  $\mathbf{X}$ ;
- Estimate for sparse matrix  $\hat{\mathbf{X}}$ ;

**Steps:**

- 1: Initialization: residual  $\mathbf{R}^{(0)} = \mathbf{Y}$ , support set  $\Lambda^{(0)} = \emptyset$ , iteration index  $t = 1$ .
- 2: Project residual onto measurement matrices

$$\mathbf{\Psi}^{(t)} = \mathbf{A}^H \mathbf{R}^{(t-1)} \mathbf{B}^c.$$

- 3: Find the index  $\lambda_t = [\lambda_t(1) \ \lambda_t(2)]$  such that

$$[\lambda_t(1) \ \lambda_t(2)] = \arg \max_{i,j} |\mathbf{\Psi}_{i,j}^{(t)}|.$$

- 4: Augment index set  $\Lambda^{(t)} = \Lambda^{(t-1)} \cup \lambda_t$ .
- 5: Find the new signal estimate

$$\hat{\mathbf{x}}^{(t)} = \left( \mathbf{D}^{(t)} \right)^{-1} \mathbf{d}^{(t)}$$

where  $\mathbf{D}^{(t)}$  and  $\mathbf{d}^{(t)}$  are given in (20) and (21).

- 6: Compute new residual

$$\mathbf{R}^{(t)} = \mathbf{Y} - \sum_{i=1}^t \hat{\mathbf{x}}_i^{(t)} \mathbf{A}_{\lambda_i(1)} \mathbf{B}_{\lambda_i(2)}^T.$$

- 7: Increment  $t$ . If  $t > L$  go to step 8, otherwise return to step 2.
  - 8: The support set is given by  $\Lambda = \Lambda^{(t)}$ . The  $(\lambda_i(1), \lambda_i(2))$ -th entry of the estimated matrix  $\hat{\mathbf{X}}$  is given by  $\hat{\mathbf{x}}_i^{(t)}$  for  $1 \leq i \leq t$ , while the rest of the elements are zeros.
- 

Similarly, other CS recovery algorithms, such as FISTA [22], [23], can be extended to our setting, namely to solve (19).

#### IV. DELAY-DOPPLER RECOVERY CONDITIONS

In this section, we will show that the range and Doppler parameters of radar targets can be unambiguously recovered under certain conditions in the noiseless case. Specifically, we derive the conditions with respect to the number of targets, under which  $\tilde{\mathbf{X}}$  can be unambiguously recovered by solving (19) in the sub-Nyquist regime. We begin with reformulating (19) in vector form, followed by some preliminaries on CS, and then derive the delay-Doppler recovery conditions.

##### A. Recovery condition in the sub-Nyquist regime

To derive the recovery conditions, we equivalently rewrite  $\mathbf{Y} = \mathbf{A} \mathbf{X} \mathbf{B}^T$  in vector form as [25]

$$\text{vec}(\mathbf{Y}) = (\mathbf{B} \otimes \mathbf{A}) \text{vec}(\mathbf{X}), \quad (23)$$

where the operator  $\text{vec}(\cdot)$  produces a vector by stacking columns of a given matrix and  $\otimes$  represents the Kronecker product. Correspondingly, the  $\ell_0$  “norm” minimization problem (19) becomes

$$\min \|\mathbf{x}\|_0, \quad \text{s.t. } \mathbf{y} = \mathbf{T} \mathbf{x}, \quad (24)$$

by letting  $\mathbf{x} = \text{vec}(\mathbf{X})$ ,  $\mathbf{y} = \text{vec}(\mathbf{Y})$  and

$$\mathbf{T} = \mathbf{B} \otimes \mathbf{A} \quad (25)$$

in (19).

Regarding the  $\ell_0$  minimization problem (24), CS theory provides conditions for recovering  $\mathbf{x}$  with (24) by investigating the spark property of the measurement matrix  $\mathbf{T}$ . The spark of  $\mathbf{T}$ , written as  $\text{spark}(\mathbf{T})$ , is defined as the size of the smallest linearly dependent subset of columns, i.e.

$$\text{spark}(\mathbf{T}) = \min \{ \|\mathbf{x}\|_0 : \mathbf{T} \mathbf{x} = \mathbf{0}, \mathbf{x} \neq \mathbf{0} \}. \quad (26)$$

In other words, if  $\text{spark}(\mathbf{T}) = \beta$ , there exists  $\beta$  columns of  $\mathbf{T}$  which are linearly dependent, and any  $\beta - 1$  columns of  $\mathbf{T}$  are linearly independent. The following lemma [26], [27] is essential to derive the recovery condition of the  $\ell_0$  minimization problem (24).

**Lemma 1.** Assume that  $\tilde{\mathbf{x}}$  is a solution of the linear observation model  $\mathbf{T} \mathbf{x} = \mathbf{y}$ , namely  $\mathbf{T} \tilde{\mathbf{x}} = \mathbf{y}$ . Then  $\tilde{\mathbf{x}}$  is the unique optimum of (24) if and only if

$$\text{spark}(\mathbf{T}) > 2 \|\tilde{\mathbf{x}}\|_0.$$

Based on Lemma 1, we then study the spark property of the specific measurement matrix  $\mathbf{T}$  in our problem, and analyze the conditions under which the sparse vector  $\tilde{\mathbf{x}} = \text{vec}(\tilde{\mathbf{X}})$  can be unambiguously recovered by solving (24). From [25], one has

$$\text{spark}(\mathbf{T}) = \text{spark}(\mathbf{B} \otimes \mathbf{A}) = \min\{\text{spark}(\mathbf{A}), \text{spark}(\mathbf{B})\}. \quad (27)$$

In our problem,  $\|\tilde{\mathbf{x}}\|_0 = \|\tilde{\mathbf{X}}\|_0 = L$ , so that the unambiguous recovery condition becomes

$$\text{spark}(\mathbf{A}) > 2L, \quad \text{spark}(\mathbf{B}) > 2L. \quad (28)$$

For convenience, let  $\beta_A = \text{spark}(\mathbf{A})$  and  $\beta_B = \text{spark}(\mathbf{B})$ . A naive bound of  $\beta_A$  is given by

$$\beta_A \leq K + 1, \quad (29)$$

because  $\mathbf{A}$  is a  $K \times N$  matrix with  $K \leq N$  and any  $K + 1$  columns of  $\mathbf{A}$  are linearly dependent. We observe that the last block in  $\mathbf{B}$  only has  $P - Q + 1$  non-zero rows, meaning that any  $P - Q + 2$  columns from the last block are linearly dependent. As a result,

$$\beta_B \leq P - Q + 2. \quad (30)$$

Since  $\mathbf{A}$  is a partial Fourier matrix generated by selecting  $K$  rows from a  $N$ -dimension Fourier matrix indexed with the subset  $\kappa \subset \{0, \dots, N - 1\}$ ,  $\beta_A$  depends on  $\kappa$ . In [28], [29], several conditions are given to produce  $\kappa$  so that  $\mathbf{A}$  has full spark, such as:

- 1) If  $N$  is a prime number, then  $\mathbf{A}$  has full spark for any subset  $\kappa$  [30].
- 2) If  $\kappa$  is comprised of  $K$  consecutive integers, then  $\mathbf{A}$  has full spark.
- 3) For positive integers  $i$  and  $M$ , let

$$\kappa = \{i, i + M, i + 2M, \dots, i + (K - 1)M\}$$

with  $i + (K - 1)M < N$ . Then  $\mathbf{A}$  has full spark if  $M$  and  $N$  are coprime [31].

With the methods in [19], [28], [29], we can easily generate subsets  $\kappa$  to ensure that  $\mathbf{A}$  has full spark, i.e.  $\beta_A = K + 1$ . We note that when the received signal is sampled at the Nyquist rate, i.e.  $K = N$  and  $\kappa = \{0, \dots, N - 1\}$ ,  $\mathbf{A}$  becomes a full Fourier matrix and the  $N$  columns of  $\mathbf{A}$  are linearly independent. In this case,  $\beta_A = N + 1 = K + 1$ .

Next, we note that  $\mathbf{B}$  is a random matrix since each element in  $\mathbf{B}$  includes a random phase item. Then  $\beta_B$  is a random variable with respect to  $\{z[p]\}$ . Nevertheless, we can prove that  $\beta_B$  almost always equals to its upper bound given in (30). Under the assumption that the random phase item  $\phi[p]$  is generated from a uniform distribution over  $[0, 2\pi)$ , the spark of  $\mathbf{B}$ ,  $\beta_B$ , almost surely equals  $P - Q + 2$ , as indicated in the following theorem.

**Theorem 1.** *Suppose that  $\phi[p]$  is independently and uniformly distributed in  $[0, 2\pi)$ , for  $p = 0, \dots, P - 1$ . Then, with probability one,  $\beta_B = P - Q + 2$ .*

*Proof.* See Appendix.  $\square$

Combining the results on  $\beta_A$  and  $\beta_B$  with the recovery condition (28), we obtain the following theorem. Here, we remind that in (31)  $K$  is the number of samples in each PRI,  $P$  is the number of transmit pulses and  $Q$  is the ambiguity factor defined in (14).

**Theorem 2.** *Assume that 1) The subset  $\kappa$  is properly designed so that  $\mathbf{A}$  has full spark; 2) The phase terms  $\{\phi[p]\}$  are independently and uniformly distributed in  $[0, 2\pi)$ . Suppose that there exist  $L$  targets with maximal ambiguity factor  $Q$ . In the noiseless setting, the range and Doppler parameters of*

*these targets can be unambiguously recovered with probability one by solving (19) or (24) if and only if*

$$L < \min \left\{ \frac{K + 1}{2}, \frac{P - Q + 2}{2} \right\}. \quad (31)$$

*Proof.* From the assumptions, one has  $\beta_A = K + 1$  and  $\beta_B = P - Q + 2$  with probability one. The recovery condition then becomes

$$K + 1 > 2L, \quad P - Q + 2 > 2L. \quad (32)$$

The condition in (31) can be directly obtained from (32).  $\square$

The randomness of the phase codes  $\{z[k]\}$  is crucial for the derivation of Theorem 1 and 2. In a pulse-Doppler radar without phase coding in which  $z[0] = \dots = z[P - 1]$ , it can be validated that

$$\mathbf{B}_1 - \mathbf{B}_2 = \mathbf{B}_{P+1} - \mathbf{B}_{P+2}, \quad (33)$$

which means there exist 4 linearly dependent columns in  $\mathbf{B}$ . As a consequence,  $\beta_B \leq 4$  and the number of targets is bounded by  $L < 2$  from (28).

### B. Recovery condition in the Nyquist regime

In the Nyquist regime, even though a direct recovery condition with respect to the number of targets  $L$  can be given by replacing  $K$  with  $N$  in (32), the condition can be actually less tight. Since  $\mathbf{A}$  is an invertible Fourier matrix, we rewrite (19) to

$$\min \|\mathbf{X}\|_0, \quad \text{s.t.} \quad \mathbf{B}\mathbf{X}^T = \mathbf{Y}^T \mathbf{A}^c. \quad (34)$$

Let  $\mathbf{X}^T = [\mathbf{r}_0, \dots, \mathbf{r}_{N-1}]$ . The new problem in (34) can be split into multiple independent sub-problems:

$$\min \|\mathbf{r}_n\|_0, \quad \text{s.t.} \quad \mathbf{B}\mathbf{r}_n = [\mathbf{Y}^T \mathbf{A}^c]_n. \quad (35)$$

for  $n = 0, \dots, N - 1$ .

In the Nyquist regime, we recover  $\mathbf{X}$  or  $\{\mathbf{r}_n\}$  by solving (35). From Lemma 1, the corresponding recovery condition is

$$\|\mathbf{r}_n\|_0 < \beta_B / 2 = \frac{P - Q + 2}{2}, \quad 0 \leq n \leq N - 1. \quad (36)$$

The conditions in the Nyquist regime only requires that the number of targets within each reduced range resolution bin is bounded by  $(P - Q + 2)/2$ , and is much looser than that in the sub-Nyquist regime, in which the total number of targets is bounded by  $(P - Q + 2)/2$ .

We note that the upper bound of the number of targets in (36) is reduced compared to a conventional pulse Doppler radar. For a Nyquist pulse Doppler radar without range ambiguity, the matrix  $\mathbf{B}$  is invertible and the number of recoverable targets in each range resolution bin is  $P$ . In our setting, range ambiguity leads to the rank deficiency of  $\mathbf{B}$ . As a result, the observation equation is underdetermined, solved by sparse matrix recovery methods, for which the upper bound of the number of targets is given in (36).

## V. NUMERICAL EXPERIMENTS

In this section, we present some numerical experiments illustrating our proposed unambiguous range-Doppler recovery algorithm. We compare our method with the classical MPRF algorithm from [11] and examine the impact of sub-Nyquist sampling as well as range ambiguity order  $Q$  on the detection performance.

### A. Preliminaries

We consider a pulse Doppler radar transmitting a pulse train composed of  $P = 20$  pulses with PRI  $\tau = 25\mu\text{sec}$  over a CPI of  $500\mu\text{sec}$ . The baseband waveform  $h(t)$  is a linear frequency modulation pulse with bandwidth  $B_h = 20\text{MHz}$  and pulse width  $T_h = 1\mu\text{sec}$ . The number of Nyquist rate samples in each PRI is thus  $N = \tau B_h = 500$ . In the simulations, we investigate sub-Nyquist sampling by reducing the number of samples  $K$  in each PRI. We randomly select  $K < N$  frequency components and obtain the corresponding compressed Fourier series by the Xampling scheme in Fig. 2. We find that the matrix  $\mathbf{A}$  has full-rank with high probability if the frequency components are selected randomly.

We consider  $L = 5$  targets with Doppler frequencies spread uniformly at random in the appropriate unambiguous region  $\nu_l \in [0, 1/\tau)$  and delays spread uniformly at random in the ambiguous region  $\tau_l \in [0, Q\tau)$  for some ambiguity factor  $Q > 1$ .

The received signal is corrupted with additive white Gaussian noise (AWGN) with variance  $\sigma_u^2$ , band-limited to  $B_h$ . We add Gaussian noise  $u(t)$  to the received signal  $y(t)$  in (5). The total transmit SNR of the transmitted pulse train is defined as

$$\text{SNR} = \frac{P \int_0^{T_h} |h(t)|^2 dt}{\sigma_u^2}. \quad (37)$$

In the simulations, the echoes of all targets have unit amplitude, i.e.  $|\alpha_l| = 1$ , for  $l = 0, \dots, L - 1$ . We use a hit-or-miss criterion as performance metric. A ‘‘hit’’ is defined as a delay-Doppler estimate circumscribed by an ellipse around the true target position in the time-frequency plane. We use ellipses with axes equivalent to  $\pm 1$  times the delay and Doppler resolution bins, equal to  $1/B_h = 50\text{nsec}$  and  $1/(P\tau) = 2\text{KHz}$ , respectively.

We compare our approach to the popular MPRF method of [11] that has been shown to outperform the matching interval scheme based on the Chinese Remainder Theorem. For the MPRF method, the pulse Doppler radar transmits two pulse trains with baseband signal  $h(t)$ . The first train is composed of  $P_1 = 20$  pulses, with PRI  $\tau_1 = 25\mu\text{sec}$  over a CPI of  $500\mu\text{sec}$ . The second train is composed of  $P_2 = 25$  pulses, with PRI  $\tau_2 = 20\mu\text{sec}$  over a CPI of  $500\mu\text{sec}$ . Like the random phase coded pulses, the observation model in (16) still holds for each pulse train in the MPRF scheme, where the measurement matrix  $\mathbf{B}$  is constructed for  $Q = 1$  and all  $z[p] = 1$ . We use Algorithm 1 to recover the ambiguous delay-Doppler map from each pulse train. Once the targets’ Doppler frequencies and ambiguous delays are recovered, we apply the clustering

method in [11] to estimate the unambiguous delays. The total transmit SNR of the two transmit pulse trains is defined as

$$\text{SNR} = \frac{(P_1 + P_2) \int_0^{T_h} |h(t)|^2 dt}{\sigma_u^2}. \quad (38)$$

Performance of RPPC and MPRF is compared with the same range resolution, Doppler resolution, total transmit SNR and number of Nyquist samples in a pulse train so that the comparison is fair.

### B. Numerical Results

In the following experiments, we investigate the delay-Doppler recovery performance of both MPRF and RPPC with respect to SNR for an ambiguous factor  $Q = 4$ . Figure 3 presents results obtained in both Nyquist and sub-Nyquist regimes. In the sub-Nyquist regime, we randomly choose  $K = 250$  and  $K = 125$  Fourier coefficients in each PRI, leading to a compression ratio of 50% and 25%, respectively. As Fig. 3 shows, the hit rate increases with the increase of the total transmit SNR, which is proportional to the SNR after matched filter in fast and slow time. We observe that our RPPC approach outperforms the MPRF approach in both Nyquist and sub-Nyquist regimes, in terms of the hit rate under the same total transmit SNR. The explanation is that the RPPC approach jointly processes all the received samples, while the MPRF approach processes the received samples of the two pulse trains separately. Therefore, the RPPC approaches can obtain better SNR after fast and slow time matched filter with the same total transmit SNR.

To achieve the same hit rate as the MPRF approach, our RPPC approach requires a lower total transmit SNR, leading to around 3dB SNR gain. As a result, for a radar transmit system with fixed pulse width, peak power and PRF, our RPPC approach needs a lower number of transmit pulses to achieve a commensurate performance with the MPRF approach, and thus reduces the cost of power and transmit time.

The impact of sub-Nyquist sampling is also demonstrated in Fig. 3. It is observed that the recovery performance in the Nyquist regime is better than that in the sub-Nyquist regime, and the recovery performance in sub-Nyquist regime decreases as the number of samples decreases.

Next, we examine the impact of the ambiguity factor  $Q$  on the delay-Doppler recovery performance of our RPPC algorithm in the sub-Nyquist regime under a compression ratio of 50%. In Fig. 4, we observe that the detection performance of our RPPC algorithm degrades slightly with increasing  $Q$  when the recovery condition from (32) holds, i.e.  $Q < 12$ , and the performance loss is more significant when  $Q > 12$ . In our signal model, the last  $Q - 1$  echoed pulses from the targets may not be received and processed, leading to a loss of SNR after matched filter in slow time. As  $Q$  increases, the SNR after matched filter becomes lower, and thus the detection performance degrades. To examine the impact of  $Q$ , we use a rather low number of pulses  $P$  in our simulation. In practical radar systems, it generally holds that  $Q \ll P$  and the performance loss caused by SNR loss is negligible.

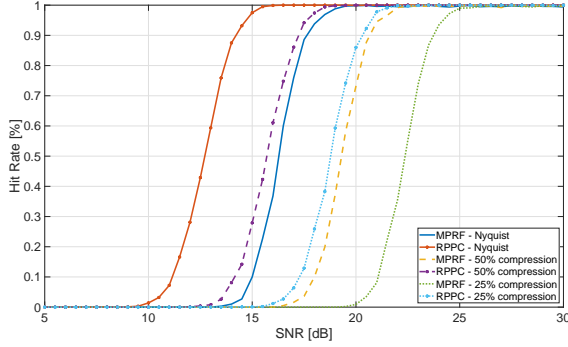


Fig. 3. Delay-Doppler recovery performance for MPRF and RPPC in Nyquist and sub-Nyquist regimes.

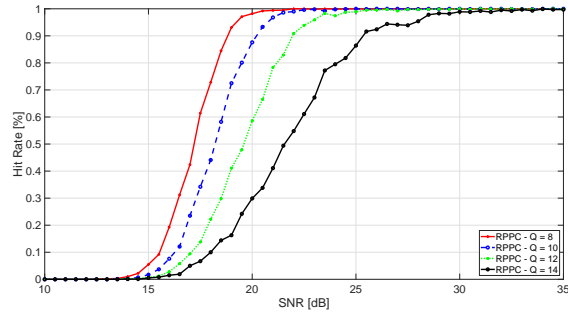


Fig. 4. Impact of the ambiguity factor  $Q$  on RPPC delay-Doppler recovery in the sub-Nyquist regime.

## VI. CONCLUSION

In this paper, a random pulse phase coding approach is proposed to resolve the range ambiguity of pulse-Doppler radars. The advantage of our approach is that the samples from all pulses can be jointly processed to estimate the range-Doppler parameters, and thus the SNR is improved. We provide a OMP based range-Doppler recovery algorithm which can be used in both Nyquist and sub-Nyquist regimes, and derive the minimal number of samples and transmit pulses for a given maximal range ambiguity order and a given number of targets. Simulation results show that our approach outperforms the MPRF method in terms of detection rate, in both Nyquist and sub-Nyquist regimes.

### APPENDIX PROOF OF THEOREM 1

Under the assumption that  $\phi[p]$  is independently and uniformly distributed in  $[0, 2\pi)$ , we will prove that  $\beta_B = P - Q + 2$  with probability one. Since  $\beta_B \leq P - Q + 2$ , we need to prove that  $\beta_B \geq P - Q + 2$ , namely any  $P - Q + 1$  columns of  $\mathbf{B}$  are linearly independent.

Let  $\overline{\mathbf{B}}$  be the matrix consisting of the  $(Q - 1)$ -th to the  $(P - 1)$ -th rows in  $\mathbf{B}$ . In the rest of the proof, we prove that it holds with probability one that any  $P - Q + 1$  columns of  $\overline{\mathbf{B}}$  are linearly independent. As a corollary, any  $P - Q + 1$  columns of  $\mathbf{B}$  are linearly independent with probability one.

For convenience, we use the following notations. Let  $u = P - Q + 1$ . Define

$$\mathcal{C} = \{(c_0, c_1, \dots, c_{u-1}) \mid 0 \leq c_0 < c_1 < \dots < c_{u-1} \leq PQ - 1\}, \quad (39)$$

which consists of all the  $u$ -combinations of the column index set  $\{0, \dots, PQ - 1\}$  for  $\overline{\mathbf{B}}$ . For each  $\mathbf{c} = (c_0, \dots, c_{u-1}) \in \mathcal{C}$ , we stack the  $c_0$ -th,  $c_1$ -th, ..., and the  $c_{u-1}$ -th columns of  $\overline{\mathbf{B}}$  into a square matrix  $\mathbf{D}(\mathbf{c})$ . Let  $c_v = Pq_v + p_v$ , where  $q_v$  is an integer in  $[0, Q - 1]$ ,  $p_v$  is an integer in  $[0, P - 1]$ , and  $q_0 \leq q_1 \leq \dots \leq q_{u-1}$ , for  $v = 0, \dots, u - 1$ . Then the  $(b - Q + 1, v)$ -th entry of  $\mathbf{D}(\mathbf{c})$  is given by  $W_P^{b p_v} z[b - q_v]$ , for  $b = Q - 1, \dots, P - 1$  and  $v = 0, \dots, u - 1$ .

The columns of a square matrix are linearly independent if and only if the determinant of the matrix is not zero. Therefore, the statement that any  $P - Q + 1$  columns of  $\overline{\mathbf{B}}$  are linearly independent is equivalent to any of the following two statements:

- (1) For any  $\mathbf{c} \in \mathcal{C}$ ,  $f(\mathbf{z}; \mathbf{c}) = \det(\mathbf{D}(\mathbf{c})) \neq 0$ .
- (2)  $F(\mathbf{z}) = \prod_{\mathbf{c} \in \mathcal{C}} f(\mathbf{z}; \mathbf{c}) \neq 0$ .

Here,  $\mathbf{z} = (z[0], \dots, z[P - 1]) = (e^{j\phi[0]}, \dots, e^{j\phi[P-1]})$ , for  $p = 0, \dots, P - 1$ .

We note that both  $F(\mathbf{z})$  and  $f(\mathbf{z}; \mathbf{c})$  can be expressed as a polynomial with respect to  $\mathbf{z}$ . To prove that any  $P - Q + 1$  columns of  $\overline{\mathbf{B}}$  are linearly independent with probability one, we only need to prove that  $F(\mathbf{z}) \neq 0$  with probability one.

To finish the proof, we first prove that  $f(\mathbf{z}; \mathbf{c})$  is a nonzero polynomial, as stated in Lemma 2. As an immediate consequence of Lemma 2,  $F(\mathbf{z})$  should be a nonzero polynomial, namely there exists  $\mathbf{z} \in \mathbb{C}^P$  satisfying that  $F(\mathbf{z}) \neq 0$ . Later in Lemma 3, we prove a strengthened version of the well-known fact that the Harr measure of the zeros of a nonzero polynomial is zero. Combining Lemma 2 and Lemma 3, since  $F(\mathbf{z})$  is a nonzero polynomial, the Harr measure of its zeros is zero. Therefore, the probability for  $F(\mathbf{z}) = 0$  is zero, and  $F(\mathbf{z}) \neq 0$  with probability one.

We start the proof by presenting Lemma 2.

**Lemma 2.** For any  $\mathbf{c}$  in  $\mathcal{C}$ ,  $f(\mathbf{z}; \mathbf{c}) = \det(\mathbf{D}(\mathbf{c}))$  is a nonzero polynomial, namely there exists  $\mathbf{z} \in \mathbb{C}^P$  such that  $f(\mathbf{z}; \mathbf{c}) \neq 0$ .

*Proof.* We note that the  $v$ -th columns of  $\mathbf{D}(\mathbf{c})$  is selected from the  $q_v$ -th block of  $\overline{\mathbf{B}}$ , for  $v = 0, \dots, u - 1$ . We first prove the proposition under the condition that all columns of  $\mathbf{D}(\mathbf{c})$  are from the same block in  $\overline{\mathbf{B}}$ , and then prove the proposition under the opposite condition. Correspondingly, the proof is divided into the two following situations:

- (a)  $q_0 = q_1 = \dots = q_{u-1}$ ;
- (b)  $q_0, q_1, \dots, q_{u-1}$  are not all the same.

*Proof for situation (a):* In this case, the  $(b - Q + 1, v)$ -th entry of  $\mathbf{D}(\mathbf{c})$  is  $W_P^{b p_v} z[b - q_0]$  and  $p_0 < p_1 < \dots < p_{u-1}$ . To calculate  $f(\mathbf{z}; \mathbf{c})$ , the determinant of  $\mathbf{D}(\mathbf{c})$ , we apply the following operations to  $\mathbf{D}(\mathbf{c})$ : First divide the  $(b - Q + 1)$ -th row by  $z[b - q_0]$  and then divide the  $v$ -th column by  $W_P^{p_v(Q-1)}$ , for  $b = Q - 1, \dots, P - 1$  and  $v = 0, \dots, u - 1$ . These operations result in a new matrix, denoted by  $\hat{\mathbf{D}}(\mathbf{c})$ , whose  $(b', v)$ -th entry is given by  $[\hat{\mathbf{D}}(\mathbf{c})]_{b', v} = W_P^{b' p_v}$ , for  $b' = 0, \dots, u - 1$



and  $v = 0, \dots, u-1$ . According to the property of determinant [32], one has

$$f(\mathbf{z}; \mathbf{c}) = \det(\hat{\mathbf{D}}(\mathbf{c})) \prod_{b=Q-1}^{P-1} z[b - q_0] \prod_{v=0}^{u-1} W_P^{p_v(Q-1)}. \quad (40)$$

We note that  $\hat{\mathbf{D}}(\mathbf{c})$  is a Vandermonde matrix and its determinant is not zero since its bases  $W_P^{p_0}, \dots, W_P^{p_{u-1}}$  are distinct [28]. Therefore,  $f(\mathbf{z}; \mathbf{c})$  is certainly a nonzero polynomial.

*Proof for situation (b):* Since the values of  $q$  are not identical, we have  $Q \geq 2$ . The proposition can be proved by mathematical induction for situation (b).

First, we check the proposition when  $\mathbf{D}(\mathbf{c}) \in \mathbb{C}^{u \times u}$  has a low dimension, say,  $u = 2$ . In this case, one has  $Q = P - 1$ ,  $\mathbf{c} = (c_0, c_1)$ ,  $P - 2 \leq b \leq P - 1$ , and we let  $q_0 < q_1$ . Then,  $\mathbf{D}(\mathbf{c})$  is written as

$$\mathbf{D}(\mathbf{c}) = \begin{bmatrix} W_P^{(P-2)p_0} z[P-2-q_0] & W_P^{(P-2)p_1} z[P-2-q_1] \\ W_P^{(P-1)p_0} z[P-1-q_0] & W_P^{(P-1)p_1} z[P-1-q_1] \end{bmatrix},$$

with its determinant  $f(\mathbf{z}; \mathbf{c})$  given by

$$f(\mathbf{z}; \mathbf{c}) = W_P^{(P-2)p_0} W_P^{(P-1)p_1} z[P-1-q_1] z[P-2-q_0] - W_P^{(P-1)p_0} W_P^{(P-2)p_1} z[P-2-q_1] z[P-1-q_0],$$

which implies that  $f(\mathbf{z}; \mathbf{c}) \equiv 0$  if and only if

$$\ell(\mathbf{z}) = \frac{z[P-1-q_1] z[P-2-q_0]}{z[P-2-q_1] z[P-1-q_0]} \equiv W_P^{p_0 - p_1}.$$

We note that  $P-1-q_1 \neq P-2-q_1$  and  $P-1-q_1 \neq P-1-q_0$ , so  $\ell(\mathbf{z})$  should not be a constant polynomial. Hence,  $\ell(\mathbf{z}) \neq W_P^{p_0 - p_1}$  and  $f(\mathbf{z}; \mathbf{c}) \neq 0$ .

Next, suppose that the proposition holds for  $u = 2, 3, \dots, u' - 1$ , or equivalently  $Q = P - 1, \dots, Q' + 1$ , where  $Q' = P - u' + 1$  and  $2 \leq Q' \leq P - 2$ . We need to prove that it holds for  $u = u'$  or  $Q = Q'$ . To this aim, we recall that  $q_0 \leq q_1 \leq \dots \leq q_{u-1}$  because  $c_0 < c_1 < \dots < c_{u-1}$ . Since  $q_0, q_1, \dots, q_{u-1}$  are not all the same, there exists an integer  $t$  satisfying that  $q_0 = \dots = q_{t-1}$  and  $q_{t-1} < q_t$ , where  $1 \leq t \leq u' - 1$ . We discuss two cases,  $t = 1$  and  $t > 1$ , in the sequel.

If  $t = 1$ , namely  $q_0 < q_1$ , only the  $(u' - 1, 0)$ -th entry of  $\mathbf{D}(\mathbf{c})$  depends on  $z[P - 1 - q_0]$ . With the Laplace's formula for determinants [32], we express the determinant of  $\mathbf{D}(\mathbf{c})$  as

$$\begin{aligned} f(\mathbf{z}; \mathbf{c}) &= \sum_{v=0}^{u'-1} [\mathbf{D}(\mathbf{c})]_{u'-1, v} C_{u'-1, v} \\ &= W_P^{(P-1)p_0} z[P-1-q_0] C_{u'-1, 0} + e(\mathbf{z}; \mathbf{c}), \end{aligned} \quad (41)$$

where  $C_{u'-1, v}$  represents the cofactor [32] of the  $(u' - 1, v)$ -entry in  $\mathbf{D}(\mathbf{c})$ , and

$$e(\mathbf{z}; \mathbf{c}) = \sum_{v=1}^{u'-1} [\mathbf{D}(\mathbf{c})]_{u'-1, v} C_{u'-1, v}. \quad (42)$$

Since only the  $(u' - 1, 0)$ -th entry of  $\mathbf{D}(\mathbf{c})$  depends on  $z[P - 1 - q_0]$ , the polynomial  $e(\mathbf{z}; \mathbf{c})$  is independent of  $z[P - 1 - q_0]$ . As a corollary,  $f(\mathbf{z}; \mathbf{c})$  is a nonzero polynomial if  $C_{u'-1, 0}$  is a nonzero polynomial.

Hence, we then prove that  $C_{u'-1, 0}$  is a nonzero polynomial with the induction hypothesis for  $Q = Q' + 1$ . We write  $\mathbf{D}(\mathbf{c})$  in block matrix form

$$\mathbf{D}(\mathbf{c}) = \begin{bmatrix} \vdots & \mathbf{E}(\mathbf{c}) \\ W_P^{-(P-1)p_0} z[P-1-q_0] & \dots \end{bmatrix}, \quad (43)$$

where  $\mathbf{E}(\mathbf{c})$  is a  $(u' - 1)$ -dimension square matrix, and then  $C_{u'-1, 0}$  can be expressed as

$$C_{u'-1, 0} = (-1)^{u'-1} \det(\mathbf{E}(\mathbf{c})). \quad (44)$$

The matrix  $\mathbf{E}(\mathbf{c})$  has a similar expression with  $\mathbf{D}(\mathbf{c})$  and the  $(b - Q', v)$ -th entry of  $\mathbf{E}(\mathbf{c})$  is  $W_P^{(b-1)p_{v+1}} z[b - 1 - q_{v+1}]$ , for  $b = Q', \dots, P - 1$  and  $v = 0, \dots, u' - 2$ . Let  $\hat{q}_v = 1 + q_{v+1}$  and  $\hat{p}_v = p_{v+1}$ . Multiply the  $v$ -th column of  $\mathbf{E}(\mathbf{c})$  by  $W_P^{\hat{p}_v}$ , for  $v = 0, \dots, u' - 2$ , and the result is a new matrix  $\hat{\mathbf{E}}(\mathbf{c})$  whose  $(b - (Q' + 1) + 1, v)$ -th entry is given by  $W_P^{b\hat{p}_v} z[b - \hat{q}_v]$ , for  $b = (Q' + 1) - 1, \dots, P - 1$  and  $v = 0, \dots, u' - 2$ . One can observe that  $\hat{\mathbf{E}}(\mathbf{c})$  has a consistent expression with  $\mathbf{D}(\mathbf{c})$  while its dimension is less than  $\mathbf{D}(\mathbf{c})$ . Using the induction hypothesis for  $Q = Q' + 1$ , the determinant of  $\hat{\mathbf{E}}(\mathbf{c})$  is a nonzero polynomial of  $\mathbf{z}$ . As a corollary,  $\det(\mathbf{E}(\mathbf{c}))$  and  $C_{u'-1, 0}$  are also nonzero polynomials, completing the proof for  $t = 1$ .

If  $t > 1$ , with the Leibniz formula [32], the determinant of  $\mathbf{D}(\mathbf{c})$  is expressed as

$$\begin{aligned} f(\mathbf{z}; \mathbf{c}) &= \sum_{\mathbf{v} \in \mathcal{S}} \text{sgn}(\mathbf{v}) \prod_{i=0}^{u'-1} \mathbf{D}_{i, v_i}(\mathbf{c}) \\ &= \sum_{\mathbf{v} \in \mathcal{S}} \text{sgn}(\mathbf{v}) \prod_{i=0}^{P-Q'} W_P^{(i+Q'-1)p_{v_i}} z[i + Q' - 1 - q_{v_i}], \end{aligned} \quad (45)$$

where the sum is computed over all the permutations  $\mathbf{v}$  for  $\{0, 1, \dots, P - Q'\}$ , and  $\mathcal{S}$  is the set consisting of all such permutations. For each permutation  $\mathbf{v}$ ,  $\text{sgn}(\mathbf{v})$  is the sign of  $\mathbf{v}$ . If  $\mathbf{v}$  can be obtained by interchanging two elements in  $(0, 1, \dots, P - Q')$  for an even number of times,  $\text{sgn}(\mathbf{v}) = 1$ . Otherwise,  $\text{sgn}(\mathbf{v}) = -1$ .

We note that  $f(\mathbf{z}; \mathbf{c})$  is expressed as the sum of several monomials. These monomials can be divided into two groups, according to whether the monomial includes the variables  $z[P - 1 - q_0], \dots, z[P - t - q_0]$ . We denote the sum of the monomials which include  $z[P - 1 - q_0], \dots, z[P - t - q_0]$  by  $f_1(\mathbf{z}; \mathbf{c})$ , and denote the sum of the monomials which do not include them or only include part of them by  $f_2(\mathbf{z}; \mathbf{c})$ . It is clear that  $f(\mathbf{z}; \mathbf{c}) = f_1(\mathbf{z}; \mathbf{c}) + f_2(\mathbf{z}; \mathbf{c})$ . Hereinafter, we show that  $f_1(\mathbf{z}; \mathbf{c})$  is a nonzero polynomial. If  $f_1(\mathbf{z}; \mathbf{c})$  is a nonzero polynomial,  $f(\mathbf{z}; \mathbf{c})$  should be a nonzero polynomial. Otherwise, one has  $f_2(\mathbf{z}; \mathbf{c}) = -f_1(\mathbf{z}; \mathbf{c})$ , indicating that the monomials in  $f_2(\mathbf{z}; \mathbf{c})$  include  $z[P - 1 - q_0], \dots, z[P - t - q_0]$ , which is opposite to the definition of  $f_2(\mathbf{z}; \mathbf{c})$ .

For  $i < u' - t$ , it holds that

$$i + Q' - 1 - q_{v_i} < u' - t + Q' - 1 - q_0 = P - t - q_0. \quad (46)$$

Therefore,  $\prod_{i=0}^{u'-t-1} \mathbf{D}_{i, v_i}(\mathbf{c})$  does not include  $z[P - 1 - q_0], \dots, z[P - t - q_0]$ . For  $\mathbf{v} \in \mathcal{S}$ , if  $\prod_{i=0}^{u'-1} \mathbf{D}_{i, v_i}(\mathbf{c})$  includes  $z[P - 1 - q_0], \dots, z[P - t - q_0]$ ,  $\prod_{i=u'-t}^{u'-1} \mathbf{D}_{i, v_i}(\mathbf{c})$  should include  $z[P - 1 - q_0], \dots, z[P - t - q_0]$ , indicating that

$$i + Q' - 1 - q_{v_i} = i + Q' - 1 - q_0 \Rightarrow q_{v_i} = q_0, \quad (47)$$

and further

$$0 \leq v_i \leq t-1, \quad (48)$$

for  $u'-t \leq i \leq u'-1$ .

Let  $\mathbf{v} = [\mathbf{v}^{(1)}, \mathbf{v}^{(2)}]$ , where  $\mathbf{v}^{(1)} = (v_0, \dots, v_{u'-t-1})$  and  $\mathbf{v}^{(2)} = (v_{u'-t}, \dots, v_{u'-1})$ . From (48), we have  $\mathbf{v}^{(1)} \in \mathcal{S}_1$  and  $\mathbf{v}^{(2)} \in \mathcal{S}_2$ , where  $\mathcal{S}_1$  is the set of all the permutations of  $\{t, \dots, u'-1\}$ , and  $\mathcal{S}_2$  is the set of all the permutations of  $\{0, \dots, t-1\}$ . Then  $f_1(\mathbf{z}; \mathbf{c})$  can be expressed as

$$f_1(\mathbf{z}; \mathbf{c}) = \sum_{\mathbf{v}^{(1)} \in \mathcal{S}_1} \sum_{\mathbf{v}^{(2)} \in \mathcal{S}_2} \text{sgn}(\mathbf{v}) \prod_{i=0}^{u'-1} \mathbf{D}_{i, v_i}(\mathbf{c}) \quad (49a)$$

$$= \sum_{\mathbf{v}^{(1)} \in \mathcal{S}_1} \sum_{\mathbf{v}^{(2)} \in \mathcal{S}_2} \text{sgn}(\mathbf{v}) \prod_{i_1=0}^{u'-t-1} \prod_{i_2=u'-t}^{u'-1} \mathbf{D}_{i_1, v_{i_1}}(\mathbf{c}) \mathbf{D}_{i_2, v_{i_2}}(\mathbf{c}) \quad (49b)$$

$$= \sum_{\mathbf{v}^{(1)} \in \mathcal{S}_1} \sum_{\mathbf{v}^{(2)} \in \mathcal{S}_2} \text{sgn}(\mathbf{v}^{(1)}) \text{sgn}(\mathbf{v}^{(2)}) \times \prod_{i_1=0}^{u'-t-1} \prod_{i_2=u'-t}^{u'-1} \mathbf{D}_{i_1, v_{i_1}^{(1)}}(\mathbf{c}) \mathbf{D}_{i_2, v_{i_2+u'-t}^{(2)}}(\mathbf{c}) \quad (49c)$$

$$= \sum_{\mathbf{v}^{(1)} \in \mathcal{S}_1} \sum_{\mathbf{v}^{(2)} \in \mathcal{S}_2} \text{sgn}(\mathbf{v}^{(1)}) \text{sgn}(\mathbf{v}^{(2)}) \times \prod_{i_1=0}^{u'-t-1} \prod_{i_2=0}^{t-1} \mathbf{D}_{i_1, v_{i_1}^{(1)}}(\mathbf{c}) \mathbf{D}_{i_2+u'-t, v_{i_2}^{(2)}}(\mathbf{c}). \quad (49d)$$

Here, (49c) comes from the fact that

$$\begin{aligned} \text{sgn}(\mathbf{v}) &= \text{sgn}(\mathbf{v}^{(1)}) \text{sgn}(\mathbf{v}^{(2)}), \\ v_{i_1} &= v_{i_1}^{(1)}, \quad 0 \leq i_1 \leq u'-t-1, \\ v_{i_2} &= v_{i_2+u'-t}^{(2)}, \quad u'-t \leq i_2 \leq u'-1, \end{aligned}$$

and (49d) is obtained via replacing  $i_2$  with  $i_2 + u' - t$ .

To further explore the property of  $h_1(\mathbf{z}; \mathbf{c})$ , we express  $\mathbf{D}(\mathbf{c})$  in block matrix form

$$\mathbf{D}(\mathbf{c}) = \begin{bmatrix} \vdots & \mathbf{E}(\mathbf{c}) \\ \mathbf{G}(\mathbf{c}) & \dots \end{bmatrix}, \quad (50)$$

where  $\mathbf{G}(\mathbf{c})$  is a  $t \times t$  matrix and  $\mathbf{E}(\mathbf{c})$  is a  $(u'-t) \times (u'-t)$  matrix. According to the relationship that

$$\begin{aligned} \mathbf{D}_{i_1, v_{i_1}^{(1)}}(\mathbf{c}) &= \mathbf{E}_{i_1, v_{i_1}^{(1)}-t}(\mathbf{c}), \quad 0 \leq i_1 \leq u'-t-1, \\ \mathbf{D}_{i_2+u'-t, v_{i_2}^{(2)}}(\mathbf{c}) &= \mathbf{G}_{i_2, v_{i_2}^{(2)}}(\mathbf{c}), \quad 0 \leq i_2 \leq t-1, \end{aligned}$$

we have

$$f_1(\mathbf{z}; \mathbf{c}) = \sum_{\mathbf{v}^{(1)} \in \mathcal{S}_1} \sum_{\mathbf{v}^{(2)} \in \mathcal{S}_2} \text{sgn}(\mathbf{v}^{(1)}) \text{sgn}(\mathbf{v}^{(2)}) \times \prod_{i_1=0}^{u'-t-1} \prod_{i_2=0}^{t-1} \mathbf{E}_{i_1, v_{i_1}^{(1)}-t}(\mathbf{c}) \mathbf{G}_{i_2, v_{i_2}^{(2)}}(\mathbf{c}) \quad (51a)$$

$$= \left( \sum_{\mathbf{v}^{(1)} \in \mathcal{S}_1} \text{sgn}(\mathbf{v}^{(1)}) \prod_{i_1=0}^{u'-t-1} \mathbf{E}_{i_1, v_{i_1}^{(1)}-t}(\mathbf{c}) \right) \times \left( \sum_{\mathbf{v}^{(2)} \in \mathcal{S}_2} \text{sgn}(\mathbf{v}^{(2)}) \prod_{i_2=0}^{t-1} \mathbf{G}_{i_2, v_{i_2}^{(2)}}(\mathbf{c}) \right) \quad (51b)$$

$$= \det(\mathbf{G}(\mathbf{c})) \det(\mathbf{E}(\mathbf{c})). \quad (51c)$$

Similar to the discussion for  $t = 1$ , one can prove that  $\det(\mathbf{E}(\mathbf{c}))$  is a nonzero polynomial using the induction hypothesis for  $Q = Q' + t$ . The  $(b, v)$ -th entry of  $\mathbf{G}(\mathbf{c})$  is given by  $W_P^{-bPv} z[b - q_0]$ , for  $b = P - t, \dots, P - 1$  and  $v = 0, \dots, t - 1$ . It is clear that  $\mathbf{G}(\mathbf{c})$  has the same structure as  $\mathbf{D}(\mathbf{c})$  in the proof for situation (a). Similarly, one can prove that  $\det(\mathbf{G}(\mathbf{c}))$  is a nonzero polynomial. Since  $\det(\mathbf{G}(\mathbf{c}))$  and  $\det(\mathbf{E}(\mathbf{c}))$  are nonzero polynomials,  $f_1(\mathbf{z}; \mathbf{c})$  is a nonzero polynomial, and  $f(\mathbf{z}; \mathbf{c})$  is also a nonzero polynomial.

Now that we have proved that the proposition holds for  $Q = Q'$ . With mathematical induction, the proposition holds for all  $Q = 2, \dots, P - 1$  under situation (b). In conclusion,  $f(\mathbf{z}; \mathbf{c})$  is a nonzero polynomial under both situations (a) and (b), and the proof is complete.  $\square$

Lemma 2 shows that  $f(\mathbf{z}; \mathbf{c})$  is a nonzero polynomial for all  $\mathbf{c} \in \mathcal{C}$ . Therefore,  $F(\mathbf{z}) = \prod_{\mathbf{c} \in \mathcal{C}} f(\mathbf{z}; \mathbf{c})$  is a nonzero polynomial. We use the following lemma to prove that  $F(\mathbf{z}) \neq 0$  with probability one, which points out the fact that the Harr measure of the set composed of zeros for a nonzero polynomial is zero.

**Lemma 3.** *Let  $F(z_0, \dots, z_{P-1})$  be a nonzero complex polynomial with  $P$  variables. Define the set of zeros of  $F$*

$$\mathcal{N}_F = \{(z_0, \dots, z_{P-1}) \in \mathbb{C}^P \mid F(z_0, \dots, z_{P-1}) = 0\}. \quad (52)$$

Define the  $P$ -torus

$$\mathcal{T}^P = \underbrace{\mathcal{T}^1 \times \dots \times \mathcal{T}^1}_P, \quad \mathcal{T}^1 = \{z \in \mathbb{C} \mid |z| = 1\}, \quad (53)$$

where  $\times$  denotes the Cartesian product. Let  $\sigma^P$  be the Harr measure on  $\mathcal{T}^P$ . Then one has

$$\sigma^P(\mathcal{T}^P \cap \mathcal{N}_F) = 0. \quad (54)$$

*Proof.* The conclusion is trivial if  $F$  is a nonzero constant polynomial. In the following, we use mathematical induction to prove the proposition with non-constant polynomial  $F$ . For  $P = 1$ ,  $\mathcal{N}_F$  is a countable set, thus the proposition is trivial. Suppose that for  $P = p$  the proposition holds. For  $P = p + 1$ , we expand  $F$  by powers of  $z_0$  and write it as

$$F(z_0, \dots, z_p) = \sum_{i=0}^d f_i(z_1, \dots, z_p) z_0^i. \quad (55)$$

Since  $F \neq 0$ , we can find  $d > 0$  so that  $f_d \neq 0$ . Denote the set of zeros of  $f_d$  by  $\mathcal{O}$  and the indicator function of  $\mathcal{N}_F$  by  $\mathcal{I}$ . According to the induction hypothesis, one has

$$\sigma^P(\mathcal{T}^P \cap \mathcal{O}) = 0, \quad (56)$$

and hence

$$\begin{aligned}
& \sigma^{P+1}(\mathcal{T}^{P+1} \cap \mathcal{N}_F) \\
&= \int_{\mathcal{T}^{P+1}} \mathcal{I}(z) d\sigma^{P+1}(z) \\
&= \int_{\mathcal{T}^P} \int_{\mathcal{T}^1} \mathcal{I}(z_0, \mathbf{y}) d\sigma(z_0) d\sigma^P(\mathbf{y}) \\
&= \int_{\mathcal{T}^P \setminus \mathcal{O}} \int_{\mathcal{T}^1} \mathcal{I}(z_0, \mathbf{y}) d\sigma(z_0) d\sigma^P(\mathbf{y}) \\
&\quad + \int_{\mathcal{T}^P \cap \mathcal{O}} \int_{\mathcal{T}^1} \mathcal{I}(z_0, \mathbf{y}) d\sigma(z_0) d\sigma^P(\mathbf{y}) \quad (57) \\
&= \int_{\mathcal{T}^P \setminus \mathcal{O}} \int_{\mathcal{T}^1} \mathcal{I}(z_0, \mathbf{y}) d\sigma(z_0) d\sigma^P(\mathbf{y}) \\
&\quad + \int_{\mathcal{T}^1} \int_{\mathcal{T}^P \cap \mathcal{O}} \mathcal{I}(z_0, \mathbf{y}) d\sigma^P(\mathbf{y}) d\sigma(z_0) \\
&= \int_{\mathcal{T}^P \setminus \mathcal{O}} \int_{\mathcal{T}^1} \mathcal{I}(z_0, \mathbf{y}) d\sigma(z_0) d\sigma^P(\mathbf{y}),
\end{aligned}$$

where  $\mathbf{y} = (z_1, \dots, z_P)$  and  $\mathbf{z} = (z_0, \mathbf{y})$ . For a given  $\mathbf{y} \in \mathcal{T}^P \setminus \mathcal{O}$ ,  $f_d(\mathbf{y}) \neq 0$  and  $F$  is a polynomial with respect to  $z_0$ . Applying the conclusion for  $P = 1$ , one has

$$\int_{\mathcal{T}^1} \mathcal{I}(z_0, \mathbf{y}) d\sigma(z_0) = 0, \text{ if } \mathbf{y} \in \mathcal{T}^P \setminus \mathcal{O}, \quad (58)$$

and hence

$$\sigma^{P+1}(\mathcal{T}^{P+1} \cap \mathcal{N}_F) = \int_{\mathcal{T}^P \setminus \mathcal{O}} \int_{\mathcal{T}^1} \mathcal{I}(z_0, \mathbf{y}) d\sigma(z_0) d\sigma^P(\mathbf{y}) = 0. \quad (59)$$

Therefore, it is proved that the proposition holds for  $P = p + 1$ . With mathematical induction, one has that the proposition holds for all positive integers  $P$ .  $\square$

From Lemma 3, one has  $\sigma^P(\mathcal{T}^P \cap \mathcal{N}_F) = 0$ . Here,  $\mathcal{N}_F$  is the set of zeros of  $F(z)$  defined in (52),  $\mathcal{T}^P$  is the  $P$ -torus defined in (53) and  $\sigma^P$  is the Harr measure on  $\mathcal{T}^P$ . Define the map  $\Theta : [0, 2\pi)^P \rightarrow \mathcal{T}^P$  by  $\Theta(\phi_0, \dots, \phi_{P-1}) = (e^{-j\phi_0}, \dots, e^{-j\phi_{P-1}})$ . The map  $\Theta$  is bijective and absolutely continuous. Let  $\mu^P$  be the Harr measure on  $[0, 2\pi)^P$ . Then one has

$$\mu^P(\Theta^{-1}(\mathcal{T}^{P+1} \cap \mathcal{N}_F)) = 0. \quad (60)$$

If  $\phi[0], \dots, \phi[P-1]$  are independent and uniformly distributed in  $[0, 2\pi)$ , the probability of  $F(z) = 0$  is

$$\frac{\mu^P(\Theta^{-1}(\mathcal{T}^{P+1} \cap \mathcal{N}_F))}{\mu^P([0, 2\pi)^P)} = \frac{\mu^P(\Theta^{-1}(\mathcal{T}^{P+1} \cap \mathcal{N}_F))}{(2\pi)^P} = 0. \quad (61)$$

In other words,  $F(z) \neq 0$  with probability one. Further, any  $P - Q + 1$  columns of  $\mathbf{B}$  are linearly independent with probability one, completing the proof.

## REFERENCES

- [1] R. J. Doviak and D. S. Zrnić, *Doppler Radar and Weather Observations*. Academic Press, 2014.
- [2] V. N. Bringi and V. Chandrasekar, *Polarimetric Doppler Weather Radar: principles and applications*. Cambridge University Press, 2005.
- [3] A. Ferrari, C. Berenguer, and G. Alengrin, "Doppler ambiguity resolution using multiple PRF," *IEEE Transactions on Aerospace and Electronic Systems*, vol. 33, no. 3, pp. 738–751, July 1997.
- [4] V. Venkatesh, L. Li, M. McLinden, G. Heymsfield, and M. Coon, "A frequency diversity pulse-pair algorithm for extending Doppler radar velocity Nyquist range," in *2016 IEEE Radar Conference (RadarConf)*, May 2016, pp. 1–6.
- [5] A. Ludloff, N. Füchter, F. Hagedorn, M. Minker, and H. Rohling, *Doppler Processing, Waveform Design and Performance Measures for Some Pulsed Doppler and MTD-radars*, ser. AEG-Telefunken Radaranlagen. AEG-Telefunken, 1981.
- [6] M. Richards, *Fundamentals of Radar Signal Processing*, ser. Professional Engineering. McGraw-Hill, 2005.
- [7] G. M. Cleetus, "Properties of staggered PRF radar spectral components," *IEEE Transactions on Aerospace and Electronic Systems*, vol. AES-12, no. 6, pp. 800–803, Nov 1976.
- [8] A. Ferrari, G. Alengrin, and C. Theys, "Doppler ambiguity resolution using staggered PRF with a new chirp sweep-rate estimation algorithm," *IEE Proceedings - Radar, Sonar and Navigation*, vol. 142, no. 4, pp. 191–194, Aug 1995.
- [9] A. Ludloff and M. Minker, "Reliability of velocity measurement by MTD radar," *IEEE Transactions on Aerospace and Electronic Systems*, vol. AES-21, no. 4, pp. 522–528, July 1985.
- [10] M. Skolnik, *Radar Handbook, Third Edition*. McGraw-Hill Education, 2008.
- [11] G. Trunk and S. Brockett, "Range and velocity ambiguity resolution," in *The Record of the 1993 IEEE National Radar Conference*, 1993, pp. 146–149.
- [12] Q. Cao, G. Zhang, R. D. Palmer, and L. Lei, "Detection and mitigation of second-trip echo in polarimetric weather radar employing random phase coding," *IEEE Transactions on Geoscience and Remote Sensing*, vol. 50, no. 4, pp. 1240–1253, April 2012.
- [13] T. Wimalajeewa, Y. C. Eldar, and P. K. Varshney, "Recovery of Sparse Matrices via Matrix Sketching," *ArXiv e-prints*, Nov. 2013.
- [14] J. A. Tropp and A. C. Gilbert, "Signal recovery from random measurements via orthogonal matching pursuit," *IEEE Transactions on Information Theory*, vol. 53, no. 12, pp. 4655–4666, Dec 2007.
- [15] O. Bar-Ilan and Y. C. Eldar, "Sub-Nyquist radar via Doppler focusing," *IEEE Transactions on Signal Processing*, vol. 62, no. 7, pp. 1796–1811, April 2014.
- [16] E. Baransky, G. Itzhak, N. Wagner, I. Shmuel, E. Shoshan, and Y. C. Eldar, "Sub-Nyquist radar prototype: hardware and algorithm," *IEEE Transactions on Aerospace and Electronic Systems*, vol. 50, no. 2, pp. 809–822, April 2014.
- [17] D. Cohen and Y. C. Eldar, "Sub-Nyquist radar systems: Temporal, spectral, and spatial compression," *IEEE Signal Processing Magazine*, vol. 35, no. 6, pp. 35–58, Nov 2018.
- [18] Y. C. Eldar and G. Kutyniok, *Compressed Sensing: Theory and Applications*. Cambridge University Press, 2012.
- [19] Y. C. Eldar, *Sampling Theory: Beyond Bandlimited Systems*. Cambridge University Press, 2015.
- [20] M. Mishali, Y. C. Eldar, and A. J. Elron, "Xampling: Signal acquisition and processing in union of subspaces," *IEEE Transactions on Signal Processing*, vol. 59, no. 10, pp. 4719–4734, Oct. 2011.
- [21] M. Mishali, Y. C. Eldar, O. Dounaevsky, and E. Shoshan, "Xampling: Analog to digital at sub-Nyquist rates," *IET Circuits, Devices Systems*, vol. 5, no. 1, pp. 8–20, Jan. 2011.
- [22] A. Beck and M. Teboulle, "A fast iterative shrinkage-thresholding algorithm for linear inverse problems," *SIAM Journal on Imaging Sciences*, vol. 2, no. 1, pp. 183–202, 2009.
- [23] A. Y. Yang, S. S. Sastry, A. Ganesh, and Y. Ma, "Fast  $\ell_1$ -minimization algorithms and an application in robust face recognition: A review," in *2010 IEEE International Conference on Image Processing*, Sept 2010, pp. 1849–1852.
- [24] D. Cohen, D. Cohen, Y. C. Eldar, and A. M. Haimovich, "SUMMeR: Sub-Nyquist MIMO radar," *IEEE Transactions on Signal Processing*, vol. 66, no. 16, pp. 4315–4330, 2018.
- [25] S. Jögar and V. Mehrmann, "Sparse representation of solutions of Kronecker product systems," *ArXiv e-prints*, Feb. 2009.
- [26] D. L. Donoho and M. Elad, "Optimally sparse representation in general (nonorthogonal) dictionaries via  $\ell_1$  minimization," *Proceedings of the National Academy of Sciences*, vol. 100, no. 5, p. 2197, 2003. [Online]. Available: <http://www.pnas.org/content/100/5/2197.abstract>
- [27] Y. C. Eldar, *Sampling Theory: Beyond Bandlimited Systems*. Cambridge University Press, 2015.
- [28] B. Alexeev, J. Cahill, and D. G. Mixon, "Full spark frames," *Journal of Fourier Analysis and Applications*, vol. 18, no. 6, pp. 1167–1194, Dec. 2012. [Online]. Available: <https://doi.org/10.1007/s00041-012-9235-4>
- [29] H. K. Achanta, S. Biswas, B. N. Dasgupta, S. Dasgupta, M. Jacob, and R. Mudumbai, "The spark of Fourier matrices: Connections to vanishing sums and coprimeness," *Digital Signal Processing*, vol. 61, pp. 76–85, Feb. 2017. [Online]. Available: <http://www.sciencedirect.com/science/article/pii/S1051200416300938>

- [30] E. J. Candes, J. Romberg, and T. Tao, "Robust uncertainty principles: exact signal reconstruction from highly incomplete frequency information," *IEEE Transactions on Information Theory*, vol. 52, no. 2, pp. 489–509, Feb. 2006.
- [31] M. E. Domínguez-Jiménez, N. González-Prelcic, G. Vazquez-Vilar, and R. López-Valcarce, "Design of universal multicoset sampling patterns for compressed sensing of multiband sparse signals," in *2012 IEEE International Conference on Acoustics, Speech and Signal Processing (ICASSP)*, March 2012, pp. 3337–3340.
- [32] K. Hoffman and R. Kunze, *Linear Algebra (2nd Edition)*. Englewood Cliffs, New Jersey: Prentice-Hall, Inc., 1971.